NURETH14-104

ELEMENTS OF VALIDATION FOR LWRS THERMAL HYDRAULIC STUDIES WITH FLICA-OVAP

Philippe Fillion, Matteo Bucci and Anne Charmeau

CEA DEN/Saclay DM2S/SFME
Laboratoire d'Etudes Thermohydrauliques des Réacteurs
91191 Gif sur Yvette Cedex, France
philippe.fillion@cea.fr, matteo.bucci@cea.fr, anne.charmeau@cea.fr

Abstract

FLICA-OVAP is an advanced two-phase flow thermal-hydraulics code based on a full 3D subchannel approach. It is designed to analyze flows in Light Water Reactors (LWRs) cores such as PWRs, BWRs and experimental reactors. Therefore its applicability covers all ranges of operating conditions for water-cooled reactors.

This paper presents an overview of FLICA-OVAP modeling capabilities for applications in nuclear reactors design and safety analysis. A validation matrix is proposed and its results are presented. The matrix covers a wide range of selected phenomena, which are relevant for thermal-hydraulics studies. Therefore the different FLICA-OVAP physical correlations addressed in the current study include single phase and two-phase friction factors, single phase and boiling heat transfer, turbulence and critical heat flux.

Results of the FLICA-OVAP validation studies highlight the capabilities of the code to well-predict two-phase flows in Light Water Reactors for both normal operation and under accidental circumstances. Future developments as well as validation activities are also summarized.

1. Introduction

The FLICA-OVAP [1] code is being developed at the *Commissariat à l'énergie atomique et aux énergies alternatives* (CEA), France, to answer various needs in nuclear reactor core modeling. The code is based on a series of solvers that adapt to the requirements associated with analysis of different core concepts and multiple industrial and research applications.

FLICA-OVAP predecessor, FLICA-4 [2], has been largely used for nuclear core safety and design analysis: its development relied on a large verification and validation database. However, FLICA-4 is based solely on a four-equation model. Hence, the FLICA-OVAP platform has been created and developed to progressively replace FLICA-4. Several new models have been implemented in the platform: an Homogeneous Equilibrium Model (HEM), a four-equation drift flux model similar to FLICA-4's, a six-equation two-fluid model and a more general multifield model. In order to validate the new models, FLICA-OVAP benefits from FLICA-4 large

database of experiments as well as new tests. Validation of the code consists of testing all of the physical correlations used in FLICA-OVAP and assessing the calculated physical quantities compared to experimental data. In this paper, validation of the four- and six-equation model is presented. The validation matrix was built such that it could cover the widest range of operating conditions as well as conditions of accidental scenarios. Studies therefore cover both 1D and 3D flows. One dimensional test sections are single channels, heated or not. Three dimensional test sections are both bundle geometries and rectangular channels accounting for LWR assemblies and plate-type fuel reactors. Pressure and mass flux ranges of the selected experiments are representative of both Boiling Water Reactors and Pressurized Water Reactors. Plate-type experimental set-up are similar to flow channels in experimental and naval propulsion reactors. The different FLICA-OVAP physical correlations closure models addressed in the current study include single phase and two-phase friction factors, single phase and boiling heat transfer, turbulence, drift velocity and critical heat flux.

1.1. Models

1.1.1. Four-equation drift-flux model

The four-equation drift-flux model of FLICA-OVAP comes directly from FLICA-4 code [3]. To simplify the equations, the model is presented without taking into account porosity. The three balance equations for the mixture read:

• mixture mass conservation

$$\frac{\partial}{\partial t} \left(\sum_{k=\nu,\ell} \alpha_k \rho_k \right) + \nabla \cdot \left(\sum_{k=\nu,\ell} \alpha_k \rho_k \mathbf{u}_k \right) = 0, \tag{1}$$

• mixture momentum balance

$$\frac{\partial}{\partial t} \left(\sum_{k=v,\ell} \alpha_k \rho_k \mathbf{u}_k \right) + \nabla \cdot \left(\sum_{k=v,\ell} \alpha_k \rho_k \mathbf{u}_k \otimes \mathbf{u}_k \right) + \nabla P - \nabla \cdot \left(\sum_{k=v,\ell} \alpha_k \underline{\underline{\tau}_k} \right) = \rho \mathbf{g} + \mathbf{F}_w$$
 (2)

mixture energy balance

$$\frac{\partial}{\partial t} \left(\sum_{k=\nu,\ell} \alpha_k \rho_k E_k \right) + \nabla \cdot \left(\sum_{k=\nu,\ell} \alpha_k \rho_k H_k \mathbf{u}_k \right) - \nabla \cdot \left(\sum_{k=\nu,\ell} \alpha_k \mathbf{q}_k \right) = q_w + \rho \mathbf{g} \cdot \mathbf{u}$$
(3)

In these equations, α_k , ρ_k , \mathbf{u}_k , E_k , H_k are respectively volume fraction, density, velocity, total energy and total enthalpy for the phase k. P is the pressure, $\rho = \sum_{k=v,\ell} \alpha_k \rho_k$ the mixture density, \mathbf{g} the gravity vector and \mathbf{F}_w the friction forces. $\underline{\tau}_k$ represents the viscous and Reynolds stress terms for the phase k, \mathbf{q}_k includes molecular and turbulent heat fluxes, and q_w is the volumetric source term of thermal power. Thermal disequilibrium is taken into account by an additional balance equation:

$$\frac{\partial}{\partial t}(\alpha_{\nu}\rho_{\nu}) + \nabla \cdot (\alpha_{\nu}\rho_{\nu}\mathbf{u}_{\nu}) - \nabla \cdot (K_{c}\nabla c) = \Gamma_{\nu}$$
(4)

where $c = \alpha_{\nu} \rho_{\nu} / \rho$ is the vapor concentration, K_c represents a diffusion term for the concentration and Γ_{ν} the mass exchange rate.

Drift-flux correlations. FLICA-OVAP includes several Zuber-Findlay type correlations in order to estimate the relative velocity $\mathbf{u}_r = \mathbf{u}_v - \mathbf{u}_\ell$ between vapor and liquid phases. The general form of these correlations is:

$$\mathbf{u}_{\nu} = C_0 \langle \mathbf{j} \rangle + \langle \langle \mathbf{v}_{gj} \rangle \rangle = C_0 \langle \mathbf{j} \rangle + \mathbf{V}_{gj}$$
 (5)

where C_0 is the distribution parameter, $\langle \mathbf{j} \rangle = \alpha \mathbf{u}_{\nu} + (1 - \alpha) \mathbf{u}_{\ell}$ the area-averaged total volumetric flux and \mathbf{V}_{gj} is the void-weighted area-averaged drift velocity. Chexal-Lellouche correlation [4] and a correlation derived from Ishii [5] are implemented because they are suitable for many flows conditions. For bubbly flows, the distribution parameter C_0 of the Ishii-type correlation in FLICA-OVAP has the following form:

$$C_0 = \left[C_{\infty} + (1 - C_{\infty}) \sqrt{\rho_{\nu}/\rho_{\ell}} \right] \left(1 - e^{-\zeta \alpha} \right) \tag{6}$$

where C_{∞} and ζ are constants, and the three-dimensional drift velocity is

$$\mathbf{V}_{gj} = -C_1 \left(\frac{\sigma ||\mathbf{g}|| (\rho_{\ell} - \rho_{\nu})}{\rho_{\ell}^2} \right)^{1/4} (1 - \alpha)^{\theta_G} \frac{\mathbf{g}}{||\mathbf{g}||}$$
 (7)

where C_1 , and θ_G are model constants, and σ is the surface tension.

Wall temperature. Wall temperatures are estimated on the basis of the bulk temperature and the heat transfer regime. In particular, four different regimes can be distinguished: single-phase convection heat transfer, subcooled nucleate boiling (SNB), saturated nucleate boiling (SANB) and eventually post critical heat flux heat transfer (post-CHF).

For single-phase heat transfer and subcooled nucleate boiling, bulk temperature is equal to the liquid phase temperature, whereas in saturated nucleate boiling it is the saturation temperature. The single-phase heat transfer coefficient is obtained by the Dittus-Boelter correlation. The onset of significant void (OSV), which is the transition between single-phase heat transfer and SNB can be predicted with Forster and Grief correlation [6] at low pressure or Jens and Lottes correlation [7] at high pressure. Both correlations allow estimating the minimum wall superheating required to achieve net vapor generation. Vapor generation starts when wall temperature estimated with Dittus-Boelter correlation exceeds this value. The Jens and Lottes model was used for the tests cases in the validation matrix.

In post-CHF conditions, the choice of correlation depends on the boiling characteristics, whether it is IAFB (inverted annular film boiling) or DFFB (dispersed flow film boiling). These solutions are detailed in section 2.3.

Mass transfer. In equation (4), the mass exchange Γ_{ν} is the sum of the vapor generation on the wall $\Gamma_{w\nu}$ and the evaporation or condensation within the bulk flow $\Gamma_{\nu l}$. $\Gamma_{w\nu}$ is correlated with the heat flux fraction for the vaporization χ :

$$\Gamma_{wv} = \frac{\chi q''}{h_{fg}} \cdot \frac{4}{D_{\text{heat}}}$$
 (8)

where D_{heat} is the heated diameter. $\chi = 0$ in the single-phase region, $\chi = 1$ in the fully saturated region, and

$$\chi = \frac{T_{w,lc} - T_{\text{sat}} - \Delta T_{\text{sat}}}{T_{w,lc} - T_l - \Delta T_{\text{sat}}}$$
(9)

in the subcooled boiling region, where $T_{w,lc}$ is the temperature given by the liquid convective heat transfer, and ΔT_{sat} the wall superheat given by the Forster and Greif or the Jens and Lottes correlation.

The mass exchange term $\Gamma_{\nu\ell}$ is given by:

$$\Gamma_{\nu\ell} = \frac{q_{\nu\ell}}{h_{\nu} - h_{\ell}} \tag{10}$$

where $q_{v\ell}$ is the heat transfer rate between the phases. In the two-phase region, $q_{v\ell}$ is modeled with the following in-house formulation [8]:

$$q_{\nu\ell} = K_{\nu 0} \frac{G^2}{\log(1 + \text{Re}/\text{Re}_0)} f(P, \rho, \mu_\ell, \mathbf{u}, \mathbf{u}_r) \frac{\rho c(x_{\text{eq}} - c)}{1 - c}$$

$$\tag{11}$$

where K_{v0} is a constant, G the mass flux, Re the Reynolds number, x_{eq} the equilibrium quality, and $f(P, \rho, \mu_{\ell}, \mathbf{u}, \mathbf{u}_r)$ a function depending on local conditions. This model represents either the vaporization $(x_{eq} > c)$ or the condensation $(x_{eq} < c)$. The flashing (spontaneous vaporization when only the liquid is present and superheated, i.e. $x_{eq} > 0$) is modeled by:

$$q_{\nu\ell} = K_{\nu 0} \frac{G^2}{\log(1 + \text{Re}/\text{Re}_0)} f(P, \rho, \mu_{\ell}, \mathbf{u}, \mathbf{u}_r) \rho \frac{x_{\text{eq}}^2}{1 - x_{\text{eq}}}$$
(12)

Pressure drop. Friction \mathbf{F}_w is the sum of the singular friction due to assembly grids or other pressure drops \mathbf{F}_{sing} and the distributed friction on wall $\mathbf{F}_{\text{frict}}$. Singular friction \mathbf{F}_{sing} is written as:

$$\mathbf{F}_{\text{sing}} = -\frac{1}{2}\rho \underline{\mathbf{K}}_{\text{sing}} ||\mathbf{u}||\mathbf{u}$$
 (13)

where $\underline{\underline{\mathbf{K}}}_{sing}$ is an antisymmetric tensor. Formulation of \mathbf{F}_{frict} used in these simulation is:

$$\mathbf{F}_{\text{frict}} = -\frac{1}{2D_h} \rho (f_{\text{iso}} \times f_{\text{heat}} \times f_{2\phi}) ||\mathbf{u}|| \mathbf{u}$$
(14)

where f_{iso} is the isothermal friction factor, f_{heat} the heating wall correction factor and $f_{2\phi}$ the two-phase multiplier given by:

$$f_{2\phi} = 1 + (\phi_{\ell o}^2 - 1) \left(1 + \frac{D_{\text{heat}}}{D_h} C_{\phi} \right)$$
 (15)

where $\phi_{\ell o}^2$ is the adiabatic two-phase frictional pressure drop multiplier, D_h the hydraulic diameter and C_{ϕ} a constant accounting for heat flux $q^{''}$ ($C_{\phi} = 0$ in the present validation).

Diffusion effects. The tensor $\underline{\tau_k}$ for viscous and turbulent effects is defined for each phase by:

$$\tau_k^{ij} = \mu_k (1 + M_{t,k}^{ij}) \left(\frac{\partial u_k^i}{\partial x_j} + \frac{\partial u_k^j}{\partial x_i} - \frac{2}{3} \sum_{l=x,y,z} \frac{\partial u_k^l}{\partial x_l} \delta_{ij} \right)$$
(16)

where $\mu_k M_{t,k}^{ij}$ is a turbulent viscosity (*i* and *j* account for the *x*, *y*, and *z* directions). For practical applications, turbulent viscosity is limited to the liquid phase. The anisotropic formulation used for turbulent conditions is:

$$M_{t,\ell}^{ij} = M_{t0}^{ij} \left(\text{Re} - \text{Re}_t \right)^{b_M} f_M(f_{2\phi})$$
 (17)

where $\text{Re} = GD_h/\mu_l$ is the Reynolds number, M_{t0}^{ij} , b_M and Re_t are parameters and $f_M(f_{2\phi})$ a function of the two-phase frictional multiplier.

Molecular and turbulent heat fluxes are written as:

$$\sum_{k=\nu,\ell} \alpha_k \mathbf{q}_k = \frac{\lambda_\ell}{C_{p_\ell}} (\underline{\underline{\mathbf{1}}} + \underline{\underline{\mathbf{K}}}_{t,\ell}) \nabla h_x$$
(18)

where $h_x = xh_v + (1-x)h_\ell$ is the flow enthalpy based on the quality x. Turbulent conductivity coefficients $K_{t,\ell}^{ij}$ are:

$$K_{t,\ell}^{ij} = K_{t0}^{ij} (\text{Re} - \text{Re}_t)^{b_K} f_K(f_{2\phi})$$
 (19)

where K_{t0}^{ij} , b_K and Re_t are parameters. In the following simulations, K_{t0} and K_c (see eq. (4)) are equal.

1.1.2. Six-equation two-fluid two-phase flow model

In three dimensions, mass, momentum and energy balance equations of the two-fluid two-phase flow model are:

$$\frac{\partial}{\partial t}\alpha_k \rho_k + \nabla \cdot (\alpha_k \rho_k \mathbf{u}_k) = \Gamma_k, \quad \text{with} \quad \sum_{k=\nu,\ell} \Gamma_k = 0, \tag{20}$$

$$\frac{\partial}{\partial t}(\alpha_k \rho_k \mathbf{u}_k) + \nabla \cdot (\alpha_k \rho_k \mathbf{u}_k \otimes \mathbf{u}_k) + \alpha_k \nabla P - \nabla \cdot (\alpha_k \underline{\underline{\tau}_k}) = \alpha_k \rho_k \mathbf{g} + \mathbf{F}_{wk} + \mathbf{F}_{ki} + \Gamma_k \mathbf{u}_i$$
 (21)

with $\sum_{k=\nu,\ell} \mathbf{F}_{ki} = 0$,

$$\frac{\partial}{\partial t}(\alpha_{k}\rho_{k}E_{k}) + P\frac{\partial}{\partial t}\alpha_{k} + \nabla \cdot (\alpha_{k}\rho_{k}H_{k}\mathbf{u}_{k}) - \nabla(\alpha_{k}\mathbf{q}_{k})$$

$$= \alpha_{k}\rho_{k}\mathbf{g} \cdot \mathbf{u}_{k} + \mathbf{F}_{ki} \cdot \mathbf{u}_{i} + q_{wk} + q_{ki} + \Gamma_{k}\left(h_{ki} + \frac{(\mathbf{u}_{ki})^{2}}{2}\right)$$
(22)

with $\sum_{k=v,\ell} (q_{ki} + \Gamma_k h_{ki}) = 0$.

Subscript i refers to the interfacial variables. There are three types of interfacial interactions: mass transfer terms, Γ_k , are the volumetric production or destruction rates of phase k due to phase changes. Interfacial momentum transfer terms, \mathbf{F}_{ki} , which are caused by drag forces, interfacial pressure forces, virtual mass effects or lift forces (the two latest terms are negligible). Interfacial heat transfer terms, q_{ki} . \mathbf{F}_{wk} represents the wall friction for the phase k and q_{wk} is the power density transferred from the wall to phase k.

The mass transfer term Γ_{ν} is:

$$\Gamma_{\nu} = \frac{-\sum_{k=\nu,\ell} q_{ki} + \sum_{k=\nu,\ell} q_{wik}}{h_{\nu i} - h_{\ell i}} + \Gamma_{res}$$
(23)

where q_{ki} is the interfacial heat transfer for phase k, q_{wik} power density transferred from the wall to phase k interface and Γ_{res} the numerical residual mass transfer rate, used in case of residual phase.

2. Validation matrix

An appropriate validation matrix is established to validate FLICA-OVAP and its various physical models for nuclear reactor applications. FLICA-OVAP main physical models have been therefore tested against the selected database. The models are:

- pressure drop model, including models for the isothermal friction factor $f_{\rm iso}$, the heating wall correction $f_{\rm heat}$ and the two-phase flow multiplier $f_{2\phi}$. The data available by CISE and those released in the frame of the BFBT benchmark have been addressed by both the four-equation and the six-equation models.
- models affecting the void fraction distribution, namely:
 - mass transfer between phases model, via K_{v0} parameter
 - drift model (C_{∞} and C_1 parameters), which also includes the effect of an angle θ ;
 - turbulence models, via turbulent conductivity K_t and turbulent mass transfer coefficient M_t

Several database are available to check the behavior of physical models in predicting void fraction distribution. Among them, the data of Bartolomei et al. are precious to assess the behavior of the drift flux model (in the four-equation model) or the interfacial friction (for the six-equation). The effect of interfacial mass transfer is assessed against the data of Bartolomei or the subchannel tests released by NUPEC for the PSBT benchmark. In bundle geometries, the relevant role of turbulent mixing and drift is assessed against experimental data released in the frame of the PSBT and BFBT benchmarks. The effects of inclination are instead checked against the DEBORA database.

 critical heat flux and post-CHF heat transfer coefficient models. Data released in the frame of the PSBT benchmark have been addressed with the four-equation model, permitting to assess the behavior of critical heat flux models in 3D bundle configurations.

Table 1: Validation matrix

Measured	1D	Parameters & Correla-	3D	Parameters & Correla-
quantities		tions		tions
Single-phase			BFBT	$f_{\rm iso}, f_{\rm heat}, \mathbf{F}_{\rm sing}$
pressure				
drops				
Two-phase	CISE	$f_{2\phi}$	BFBT	$f_{2\phi}$
pressure				
drops				
α	Bartolomei	Interfacial mass transfer model	BFBT	Interfacial mass transfer model
		Drift model (C_0 , \mathbf{V}_G)		Drift model (C_0 , \mathbf{V}_G)
		Interfacial friction (six-		Interfacial friction (six-
		equation)		equation)
				Turbulence model (K_t, M_t)
		Subcooled and saturated		Subcooled and saturated
		nucleate boiling model		nucleate boiling model
			DEBORA	Drift model in stratified
				flows
	PSBT	Drift Model	PSBT	Turbulence model (K_t , M_t)
		Mass Transfer Model		in presence of spacer and
		$(K_{v,0})$		mixing grids
				Transient scenarios
$q_{ m chf}^{''}$			PSBT	CHF correlation
				Transient scenarios
T_w	Bennett	CHF and post-CHF corre-		
		lations		

The data available by Bennett et al. have been analyzed to check the behavior of post-CHF heat transfer correlations.

Models and corresponding experimental tests for their validation are summarized in Table 1. A summary description of tests, FLICA-OVAP modeling choices and calculation results are reported in the following sections.

2.1. CISE experiments for pressure drop calculation benchmarks

CISE experiments were carried out at the Piacenza facility (CAN-2 program). Total pressure drop is measured in a vertical circular tube for an upward flow in adiabatic conditions. Measurements are performed on two test sections of variable hydraulic diameters and large spectrum of pressures, mass fluxes and qualities similar to BWRs operating conditions (see Tab. 2).

Water enters the test section at saturation temperature and there is no heating of the walls. Experimental data consist of inlet mass flux for the mixture, inlet quality as well as exit pressure

Table 2: Experimental conditions of CISE tests

Pressure [bar]	20;50;70
Pipe inside diameter [mm]	9.18; 15.3
Mass flux kg·m $^{-2}$ ·s $^{-1}$	from 110 to 3900
Flow quality	from 0.0307 to 0.9814
Length [m]	1.429 ; 2.5

and total pressure drop measured between two pressure taps. Experimental boundary conditions are input in the code: validation of FLICA-OVAP consists in comparing calculated and measured pressure drops.

The benchmark allows for the validation of both four- and six-equation models and two closure models, in particular the wall friction two-phase multiplier model and the one-dimensional interfacial friction model. Friction force for the four-equation model is given in equation (14). Since there is no external source of heat in the experiment, $f_{\text{heat}} = 1$. The isothermal friction factor depends on the flow regime. Only turbulent flows are modeled for the CISE tests, therefore, the isothermal friction factor correlation is given by Blasius's law: $f_{\text{iso}} = 0.316 \, \text{Re}^{-0.25}$. Chisholm [9] and Friedel [10] correlations of the two-phase adiabatic multiplier $\phi_{\ell o}^2$ were assessed. For the six-equation model, both interfacial friction and wall friction correlations are derived from CATHARE code [11].

The data base of 289 tests has been run with both the four-equation and the six-equation solvers. Some results are summarized in Table 3.

Table 3: Averaged calculation error on the total pressure drop calculations (P=70 bar, D_h =9.18 mm)

Model	average error(%)
four-equation, Chisholm	22.2 %
four-equation, Friedel	13.2 %
six-equation	14.4 %

At pressure 70 bar, the four-equation model with the Friedel two-phase wall friction multiplier and the six-equation model gave similar averaged errors. Chisholm correlation tends to over-predict the pressure drop and a larger error has been found with this correlation. This result confirms the recommendation of Whalley [12] for the use of the Friedel correlation when $\mu_l/\mu_g < 1000$, instead of other models including Chisholm.

The CISE benchmark exercise shows the ability of the code to model one-dimensional pressure drop for a wide variety of pressures, mass fluxes and qualities. Calculated pressure drops across the channel are in good agreement with the experimental measurements. Figure 1 for example shows the results of the FLICA-OVAP calculations in dots with comparison to experimental results in solid lines. The results are for the particular case of an operating pressure of 50 bars and calculations are done with the six-equation solver. Pressure drops are better predicted as the mass flux is high.

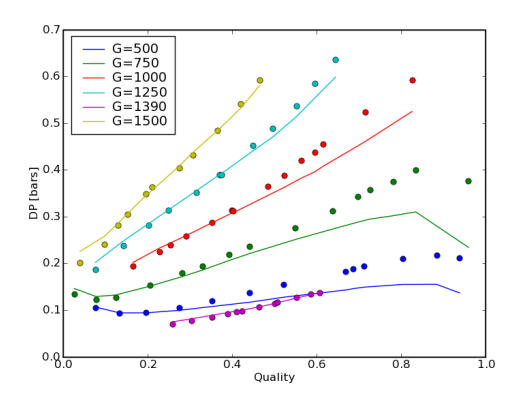


Figure 1: CISE experiment: Predicted and experimental pressure gradients against quality for different mass fluxes (pressure = 50 bars)

2.2. Bartolomei et al. experiments

Measurements of void fraction under subcooled conditions and tubular geometry were performed by G.G. Bartolomei et al. at the Moscow Power Institute [13]. These tests have the advantage of covering an operating range for the PWR from the accident conditions (pressure from 30 to 100 bar and mass flux below $1000 \text{ kg} \cdot \text{m}^{-2} \cdot \text{s}^{-1}$) to conditions approaching the nominal operation in term of pressure (pressures close to 150 bar). 24 results of void fraction profiles vs. the equilibrium quality x_{eq} are presented for different values of pressure, inlet mass flux, inlet temperature and uniform heat flux density.

For the four-equation model, these runs allow to assess the drift flux correlations (Chexal-Lellouche [4] and Ishii [5]) and the interfacial heat transfer rate $q_{v\ell}$ (Eq. 11) in subcooled boiling and in nucleate boiling for the full saturation zone. In the six-equation model, the interface to liquid heat transfer $q_{\ell i}$ in (Eq. 23), corresponding to the condensation in subcooled boiling, is evaluated from [14]:

$$q_{\ell i} = \frac{\alpha_{\nu} \rho_{\ell} C_{p_{\ell}} \Delta T_{\text{sub}}}{\tau_{0} (G_{0}/G)^{2} \log(1 + G/G_{0})} \quad \text{if} \quad T_{\ell} < T_{\text{sat}}$$
 (24)

where C_{p_l} is the liquid heat capacity, $\tau_0 = 5.37 \times 10^{-2} \text{ s}$ and $G_0 = 1000 \text{ kg} \cdot \text{m}^{-2} \cdot \text{s}^{-1}$, in the range $405 \le G \le 2123 \text{ kg} \cdot \text{m}^{-2} \cdot \text{s}^{-1}$.

Bartolomei's data have been used by several authors to assess their models in these conditions. Delhaye et al. [15] used the Saha and Zuber criterion to determine the subcooling at the onset of significant void, and the Zuber and Findlay model to calculate the void fraction, whereas Anne et al. [16] reported the assessment of the RELAP5 and CFX-4 numerical predictions at high pressure against these data.

Figure 2 shows a comparison between the four-equation model with the Chexal-Lellouche or the Ishii drift flux correlation, the six-equation model and the experimental data points. The considered drift flux correlations do not significantly affect the results for the four-equation model. However, with this model, the void fraction is underestimated in the saturated region. The six-equation model gives good agreements against the experiment for these tests.

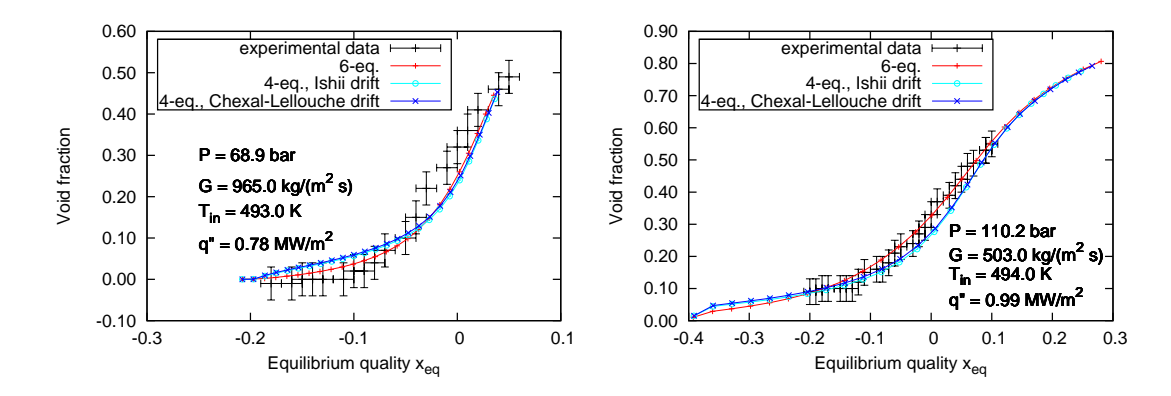


Figure 2: Comparison of the results obtained by FLICA-OVAP models and Bartolomei experimental data (P: inlet pressure, G: mass flux, T_{in} : inlet temperature, q'': heat flux)

2.3. Bennett et al. experiments

One of the most relevant database of post critical heat flux heat transfer is the one made available by Bennett et al. [17]. Experiments were carried out on the Harwell High Pressure Two Phase Heat Transfer Loop, consisting of cylindrical tubes with two different heated length.

More than 200 tests were performed, investigating different physical phenomenologies. Tests with moderate flow rates and moderate heat fluxes addressed situations of dryout with dispersed liquid droplets (high qualities), which are characterized by important thermal non-equilibrium effects between vapor and the liquid (droplets) phases. Tests with higher mass flow rates investigated phenomena approaching inverted annular film boiling conditions, typical of low quality flow and high heat fluxes, which can be reasonably described by models based on thermal equilibrium assumption.

In FLICA-OVAP, several models are implemented to predict critical heat flux conditions. The W3 correlation [18] is adapted to predict departure from nucleate boiling phenomena typical of pressurized water reactor. Dryout conditions are instead evaluated by means of the Katto [19] or the Shah [20] model. In this analysis, the location of dryout was predicted by the Shah model, which consists of two separate correlations to determine the *boiling number* Bo, defined as

$$Bo = \frac{q''_{chf}}{Gh_{\ell v}} \tag{25}$$

The first correlation covers situations where the critical heat flux depends on the upstream conditions, named UCC (*Upstream Conditions Correlation*). The second, named LCC, depends only on local quantities.

To deal with the prediction of the post critical heat flux heat transfer coefficient, two different models are currently implemented in FLICA-OVAP to be used with the four-equation model. The model of Dougall and Rohsenow [21], based on the assumption of thermal equilibrium, is adapted to analyze tests where equilibrium conditions are expected. This correlation is based on the Dittus-Boelter correlation for single phase heat transfer. The difference with single phase heat transfer is accounted for by the use of the actual mass flux in the two-phase Reynolds

number:

Nu = 0.023
$$\left[\left(\frac{GD_h}{\mu_v} \right) \left(x_{eq} + \frac{\rho_v}{\rho_\ell} (1 - x_{eq}) \right) \right]^{0.8} Pr_{v,sat}^{0.4}.$$
 (26)

To account for non-equilibrium effects, the Groeneveld and Delorme [22] model is available in FLICA-OVAP. The model allows to estimate the actual vapor quality and the actual vapor temperature in non-equilibrium conditions, simply basing on equilibrium quantities:

$$Nu = 0.008348 \left[\left(\frac{GD_h}{\mu_{\nu,f}} \right) \left(x_a + \frac{\rho_{\nu}}{\rho_{\ell}} (1 - x_a) \right) \right]^{0.8774} Pr_{\nu,f}^{0.6112}$$
(27)

where x_a and $T_{v,a}$ are the actual vapor quality and the actual vapor temperature. Nevertheless, asymptotic equilibrium conditions are recovered.

Experimental wall temperatures are compared to calculated values for tests at low void fractions and high heat flux and for tests at high void fractions and moderate heat fluxes, respectively in Figures 3 (a) and (b). The behavior of the models is qualitatively and quantitatively satisfactory in both cases. Despite the use of a four-equation equilibrium model, the model of Groeneveld and Delorme allows to achieve a satisfactory description of physical phenomena in the tests characterized by important thermal non equilibrium effects (Fig. 3 (b)).

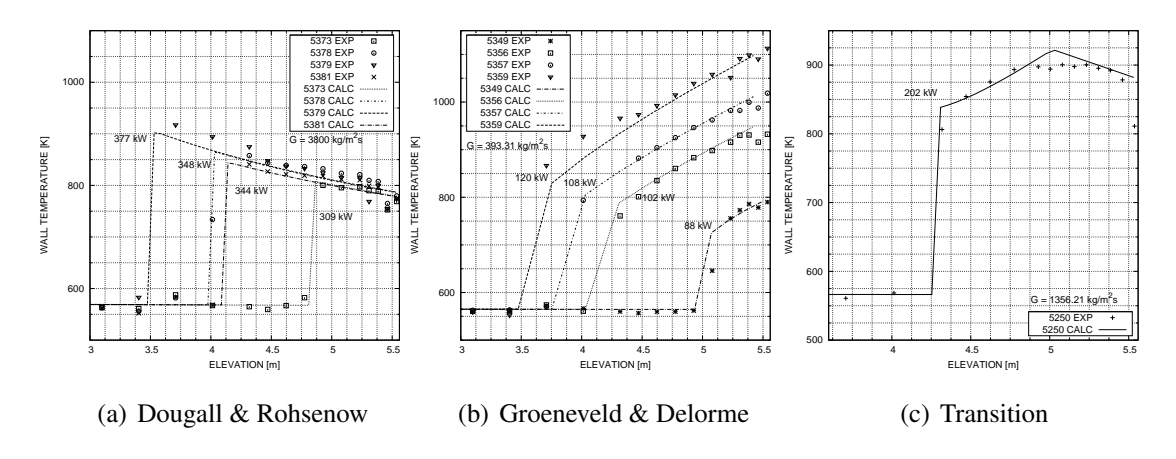


Figure 3: Comparison between experimental and calculated wall temperatures in the Bennett tests with Dougall and Rohsenow model (equilibrium conditions) (a), Groeneveld and Delorme model (non-equilibrium conditions) (b) and transition between non equilibrium and equilibrium conditions (c).

In Fig. 3 (c), sample results obtained for tests at intermediate conditions are shown. Non-equilibrium conditions are expected after the boiling crisis location where the steam and the wall temperature increase. Then, mass transfer between superheated steam and droplets occurs, permitting to evaporate droplets and cool down the steam. As a consequence the walls are also cooled down. This behavior is qualitatively reproduced by the model of Groeneveld and Delorme, even if the transition between the thermal non-equilibrium behavior and the droplet evaporation phase is sharper than reality.

2.4. OECD/NRC BFBT benchmark

The BWR Full-size Fine Mesh Bundle Tests (BFBT) benchmark [23] aimed at promoting the validation of existing thermal-hydraulics codes and encourage the development of new computational tools for the modeling of two-phase flows. Based on the data made available by the Nuclear Power Engineering Corporation (NUPEC) in Japan, the benchmark consists of several exercises including steady-state and transient void distribution tests as well as critical power tests in a full-size mock-up representative of different BWR-type assemblies (see Fig. 4).

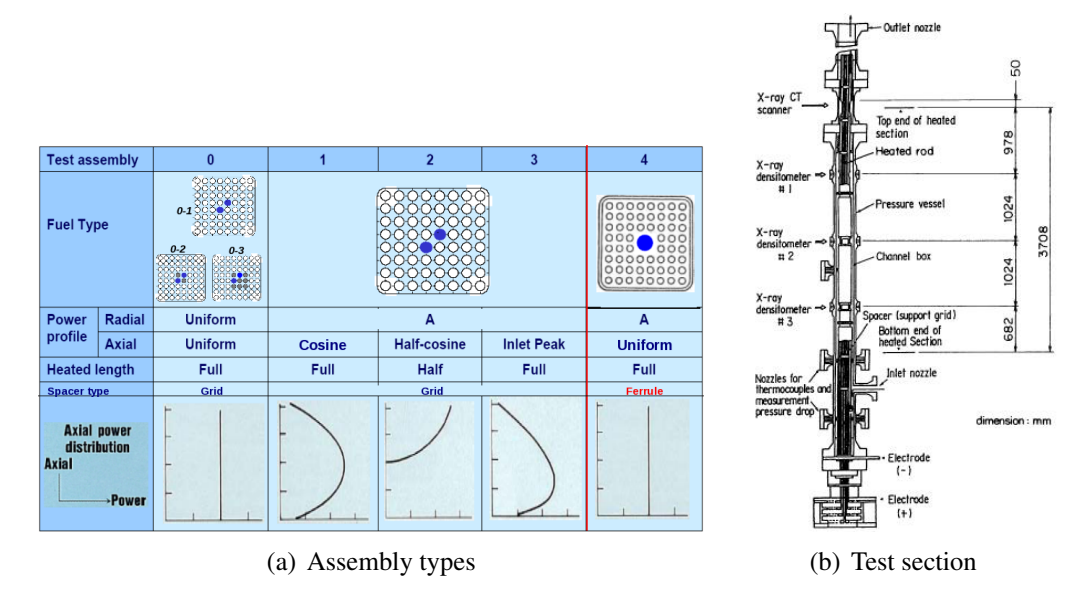


Figure 4: BFBT assembly types and test section

Among the different experimental campaigns carried out within the BFBT test section (see Fig. 4 (b)), the attention was focused on tests involving pressure drops measurements and tests where the axial void fraction profile was measured. 22 pressure drops tests and 15 void distribution tests were addressed involving radial and axial power profiles (see Fig. 4) and different operating conditions (see Tab. 4). Experimental void fraction were determined by X-ray CT scanner and X-ray densitometer at several elevations (see Fig. 4 (b)).

Table 4: Experimental conditions of the BFBT pressure drop and void distribution tests

	Pressure drop tests	Void distribution tests
Outlet pressure [MPa]	7.2;8.6	7.2
Inlet subcooling [kJ/kg]	50.2	50.2
Outlet quality [%]	7;15;25	5;12;25
Inlet mass flow rate [t/h]	20 – 50	55

One-dimensional (1D) and three-dimensional (3D) calculations of the rod bundle were performed. Both four-equation and six-equation models have been tested. In the case of the drift flux model, the analysis was aimed at assessing:

- in particular for pressure drop runs: the singular pressure drop model and the correlation to evaluate the two-phase flow multiplier;
- in particular for void distribution runs: Ishii and Chexal-Lellouche drift models in rod bundle geometries, the mass transfer model between vapor and liquid phases Γ_{vl} , the wall transfer models and the turbulence model.

In the case of the six-equation model, the analysis aimed at assessing the condensation and flashing terms, the entrainment model [11], the wall heat transfer model (the same correlations as for the four-equation model) and the pressure drop models. For the interfacial transfer term q_{ℓ_1} , the formulation (Eq. 24) has been used.

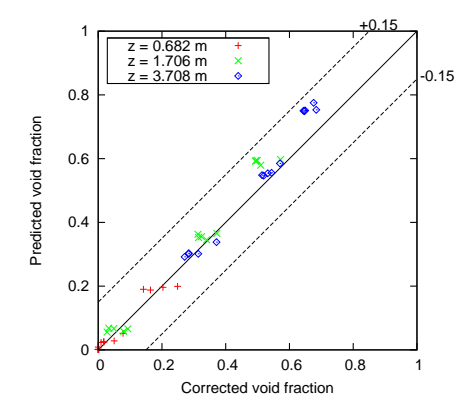


Figure 5: BFBT void distribution tests. Comparison of the predicted cross-sectional average void fraction at z = 0.682, 1.706 and 3.708 m vs. experimental corrected void fraction [24], for the six-equation model.

Calculated void fractions are compared to both experimental measurements and corrected void fractions (Fig. 5). At the bottom and the middle of the bundle, the predicted results mainly depend on the condensation term: pretty good agreement is found in this region. At the top of the bundle, the drift flux correlation or the drag is one of the key correlations to well fit the experimental data: simulation results for highest qualities tend to slightly over-predict the experimental corrected void fractions.

The accuracy of the 3D calculations for the void fraction distribution tests strongly depends on the mixing parameter M_{t0} and the conductivity parameter K_{t0} of the diffusion models. In Figure 6 the radial distribution of the void fraction error at the outlet of the test section is plotted, for the tests 0021-16 and 0031-16. Maximal error for both tests is less than 14%. For the run 0031-16, the maximal error is located near the non-heating rods where the void fraction is overestimated. Nevertheless, void fraction distribution is well predicted on the border subchannels.

2.5. PSBT benchmark

Based on NUPEC PWR Subchannel and Bundle Tests (PSBT), an international benchmark has been promoted by OECD and NRC and has been coordinated by Penn State University [25].

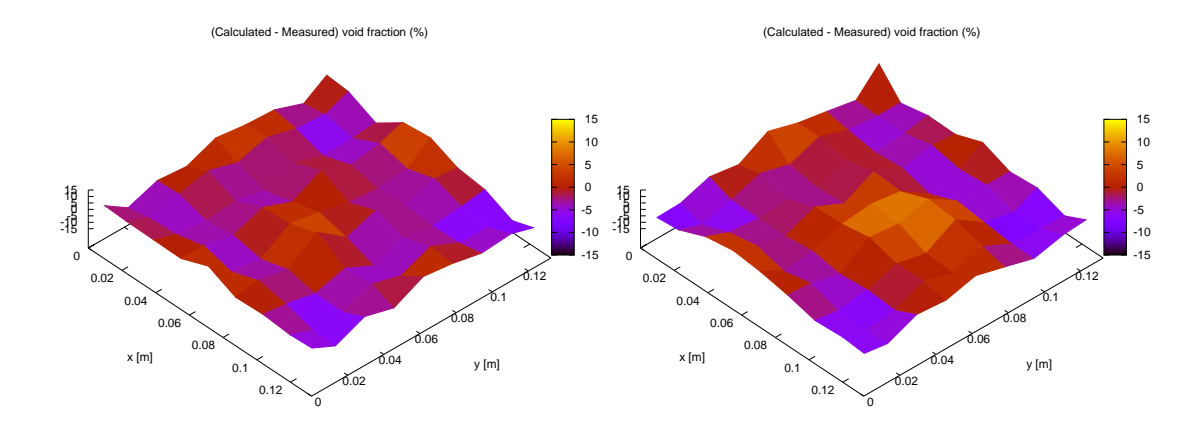


Figure 6: BFBT tests 0021-16 and 0031-16 – Error produced by the four-equation model for the outlet void fraction map with $M_{t0} = 0.019$ and $K_{t0} = 0.019$.

The aim of this benchmark is to encourage advancement and assessment of numerical models in subchannel analysis of fluid flow in rod bundles, which has very important relevance for the nuclear reactor safety margin evaluation. A important database of void fraction and critical heat flux measurements in steady-state and transient conditions have been carried out by NUPEC on a prototypical PWR rod bundle. Different types of subchannel or rod bundle geometries, and a wide range of flow conditions at high pressure have been investigated, allowing to assess the behavior of key models and correlations in these conditions.

The four-equation model have been used to simulate steady-state and transient exercises proposed by this benchmark. For void distribution rod bundle series, drift correlations, the effect of the condensation parameter $K_{\nu 0}$ and of the diffusion coefficients M_{t0} and K_{t0} in presence of mixing vane spacers have been analyzed. In DNB steady-state and transient exercises, the Shah [20] and Katto and Ohno [19] critical heat flux correlations have been assessed. The results of void fraction distribution and DNB exercises have been extensively described in [26, 27].

2.6. DEBORA experiments for validation of two-dimensional void fraction profile calculations

The DEBORA experiments were led at the CEA in the early 2000s. They were originally designed to qualify naval propulsion in-core thermal hydraulics and safety codes. The test section has a rectangular cross section and is electrically heated with two external plates (Figure 7). The experimental set-up controls inlet mass flux and inlet temperature as well as exit pressure. At the exit of the test section, two-dimensional profiles of void fraction are measured using a bi-probe. Experimental fluid is freon R12. Extensive studies have led to a valid transposition between freon and water: experiments are simulated using water as a coolant and boundary conditions for the water experiments are obtained with the transposition.

The most interesting feature of the experiments is that some of the tests are conducted with the test section held at an angle: stratification of the flow becomes predominant. Validation studies were conducted with the homogeneous four-equation model of FLICA-OVAP. Physical models used for the FLICA-OVAP simulations include two-phase friction multiplier predicted by the

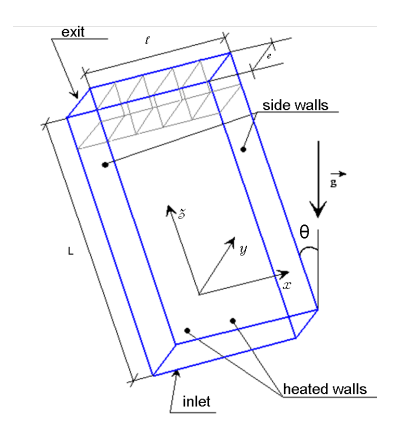


Figure 7: Test section for the DEBORA experiments

Friedel correlation, the mass transfer model between vapor and liquid Γ_{vl} and a derived form of the Ishii and Zuber drift-flux model [28] for stratified flows using a three-dimensional tensor for the distribution parameter, with optimized C_{∞} and ζ constants in the scope of naval propulsion studies.

Two-dimensional void fraction profiles at the exit of the test section are compared to experimental results. Because of the confidentiality of the results, this paper will not present in details the data that has been used. However, the results being quite interesting, they will be shown as normalized.

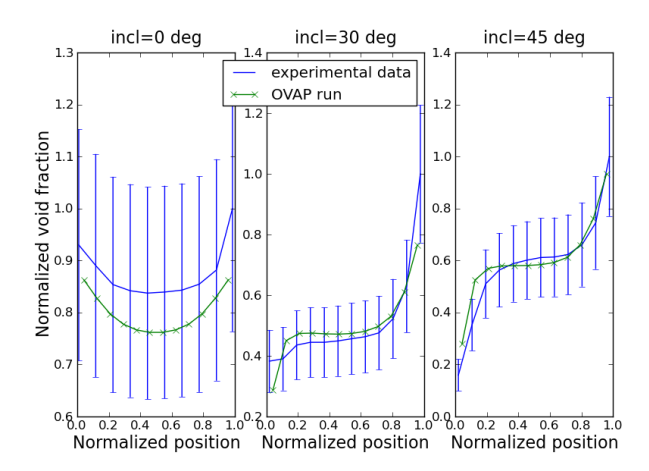


Figure 8: Normalized void fraction profiles for the DEBORA experiments, calculated with FLICA-OVAP 4-equation model

Results of three tests are shown Figure 8: subplots from left to right respectively holds for an inclination of the test section of 0° , 30° and 45° . FLICA-OVAP well predicts the two-dimensional profiles, especially in the area where stratification is the most important. This preliminary study shows the good predictability of highly stratified flows with the four-equation model. Further investigation will consist in calculation of the profiles using FLICA-OVAP six-

equation model.

3. Conclusions

FLICA-OVAP is an advanced two-phase thermal-hydraulic code designed to analyze flows in light water reactor cores. It includes a homogeneous equilibrium model, a 4 equations drift-flux model, a two-fluid six-equation model and a generic multi-field model. In this paper, the current capabilities of the four-equation and the six-equation models have been presented.

The attention has been focused on those aspects which are of major interest in the design and the safety analysis of nuclear reactors. Therefore, the models have been tested against experimental data covering a wide range of physical phenomena, including two-phase flow pressure drop, boiling heat transfer, critical heat flux and post critical heat flux heat transfer, and involving flows with both moderate and high void fractions. One- and three-dimensional geometries have been investigated. Satisfactory results have been achieved in all the proposed tests.

Future activities are presently being planned, aimed at consolidating the validation of the code. It is also planned to address the DEBORA, Bennett and PSBT tests with the two-fluid model. It could be also envisaged to apply a three-fluid model (liquid, vapor and droplets) to some post critical heat flux tests of the Bennett database.

Acknowlegments

The authors would like to thanks Alessio Pesetti, University of Pisa, Italy, for his contribution in the analysis of the Bennett database.

References

- [1] P. Fillion, A. Chanoine, S. Dellacherie, and A. Kumbaro, "FLICA-OVAP: a New Platform for Core Thermal-hydraulic Studies," in *Proceedings of NURETH-13*, Kanazawa, Japan, Sep. 26 Oct. 2 (2009).
- [2] I. Toumi, A. Bergeron, D. Gallo, E. Royer, and D. Caruge, "FLICA-4: a three-dimensional two-phase flow computer code with advanced numerical methods for nuclear application," *Nucl. Eng. Des.*, **200**, pp. 139–155, (2000).
- [3] E. Royer, S. Aniel, A. Bergeron, P. Fillion, D. Gallo, F. Gaudier, O. Grégoire, M. Martin, E. Richebois, P. Salvadore, S. Zimmer, T. Chataing, P. Clément, and F. François, "FLICA4: Status of numerical and physical models and overview of applications," in *Proceedings of NURETH-11*, Avignon, France, October 2-6 (2005).
- [4] B. Chexal, G. Lellouche, J. Horowitz, and J. Healzer, "A Void Fraction Correlation for Generalized Applications," *Progress In Nuclear Research*, **27**, no. 4, pp. 255–295, (1992).
- [5] M. Ishii, "One dimensional drift-flux model and constitutive equations for relative motion between phases in various two-phase flow," Tech. Rep. ANL-77-27, ANL, (1977).
- [6] H. Forster and R. Greif, "Heat transfer to a boiling liquid Mechanism and correlations," *J. Heat Transfer Trans. ASME*, **81**, pp. 43–53, (1959).

- [7] W. Jens and P. Lottes, "Analysis of heat transfer burnout, pressure drop and density data for high pressure water," Tech. Rep. ANL-4627, ANL, (1951).
- [8] M. Fajeau, D. Menessier, and C. Lavalée, "Méthode de calcul du taux de vide," Tech. Rep. SPM 1007, STT 68-22-E, CEA, (1968).
- [9] D.Chisholm, "Friction During the Flow of Two-Phase Mixtures in Smooth Tubes and Channels," Tech. Rep. NEL 529, National Engineering Laboratory, (1972).
- [10] L. Friedel, "Improved friction pressure drop correlations for horizontal and vertical two phase pipe flow," in *European Two Phase Flow Meeting*, Ispra, June 5-8th (1979).
- [11] P. Bazin, G. Geffraye, and G. Serre, "Physical laws of Cathare revision 6.1. Pipe Module," Tech. Rep. SMTH/LMDS/EM/2002-096, CEA, (2003).
- [12] P. B. Whalley, *Boiling, Condensation, and Gas-liquid Flow.* Oxford Science Publication, Clarendon Press, (1987).
- [13] G. G. Bartolomei, V. G. Brantov, Y. Molochnikov, and al., "An Experimental Investigation of True Volumetric Vapour Content with Subcooled Boiling in Tubes," *Therm. Eng.*, **29**, no. 3, pp. 132–135, (1982).
- [14] M. Bucci, A. Charmeau, and P. Fillion, "FLICA-OVAP: elements of validation for LWRs thermal-hydraulic studies," in *Proceedings of ICAPP 2011*, Nice, France, May 2-5 (2011).
- [15] J. M. Delhaye, F. Maugin, and J. M. Ochterbeck, "Void fraction predictions in forced convective subcooled boing of water between 10 and 18 MPa," *Int. J. Heat Mass Transfer*, **47**, pp. 4415–4425, (2004).
- [16] R. D. Anne, D. R. H. Beattie, and J. Y. Tu, "Thermal-hydraulics code validation for HIFAR fuel element safety analyses," in *13th Australasian Fluid Mechanics Conference*, Monash University, Melbourne, Australia, 13-18 dec. (1998).
- [17] A. Bennett, G. Hewitt, H. Kerseay, and R. Keeys, "Heat transfer to steam-water mixtures flowing in uniformly heated tubes in which the critical heat flux has been exceeded," Tech. Rep. AERE-R5373, Atomic Energy Research Establishment, (1967).
- [18] N. Todreas and M. Kazimi, Nuclear Systems I. Taylor & Francis.
- [19] Y. Katto and H. Ohno, "An improved version of the generalized correlation of critical heat flux for forced convective boiling in uniformly heated vertical tubes," *Int. J. Heat Mass Transfer*, **27**, no. 9, pp. 1641–1648, (1984).
- [20] M. Shah, "Improved general correlation for critical heat flux during upflow in uniformly heated vertical tubes," *Heat and Fluid Flows*, **8**, pp. 326–335, December (1987).
- [21] R. Dougall, Film Boiling on the inside of vertical tubes with upward flow of the fluid at low qualities. PhD thesis, Massachusetts, September (1963).
- [22] D. Groeneveld and G. Delorme, "Prediction of thermal non-equilibrium in the post-dryout regime," *Nucl. Eng. Des.*, **36**, pp. 17–26, (1976).
- [23] B. Neykov, F. Aydoyan, L. Hochreiter, K. Ivanov, H. Utsuno, F. Kasahara, E. Sartori, and M. Martin, "OECD-NEA/US-NRC/NUPEC BWR Full-size Fine-mesh Bundle

- Test (BFBT) Benchmark. Volume I: Specifications," Tech. Rep. NEA/NSC/DOC(2005)5, OECD Nuclear Energy Agency, (2006).
- [24] F. Aydogan, L. Hochreiter, and K. Ivanov, "Correlation for the bundle averaged void fraction measured with X-ray densitometers in the OECD/NRC BFBT benchmark," Tech. Note, OECD/NRC, Apr. 29 (2007).
- [25] A. Rubin, A. Schoedel, M. Avramava, and H. Utsuno, "OECD/NRC benchmark based on NUPEC PWR subchannel and bundle tests (PSBT). Volume I: Experimental Database and Final Problem Specifications," Tech. Rep. NEA/NSC/DOC(2010)1, NEA/NSC, Nov. (2010).
- [26] P. Fillion and M. Bucci, "Analysis of the NUPEC PBST tests with FLICA-OVAP. Part 1: void distribution benchmark," in *Proceedings of NURETH-14*, Toronto, Canada, Sep. 25-30 (2011). Submitted to.
- [27] M. Bucci and P. Fillion, "Analysis of the NUPEC PBST tests with FLICA-OVAP. Part 2: DNB benchmark," in *Proceedings of NURETH-14*, Toronto, Canada, Sep. 25-30 (2011). Submitted to.
- [28] M. Ishii and N. Zuber, "Drag coefficient and relative velocity in bubbly, dropplet or particulate flows," *AIChE Journal*, **25**, no. 5, (1979).